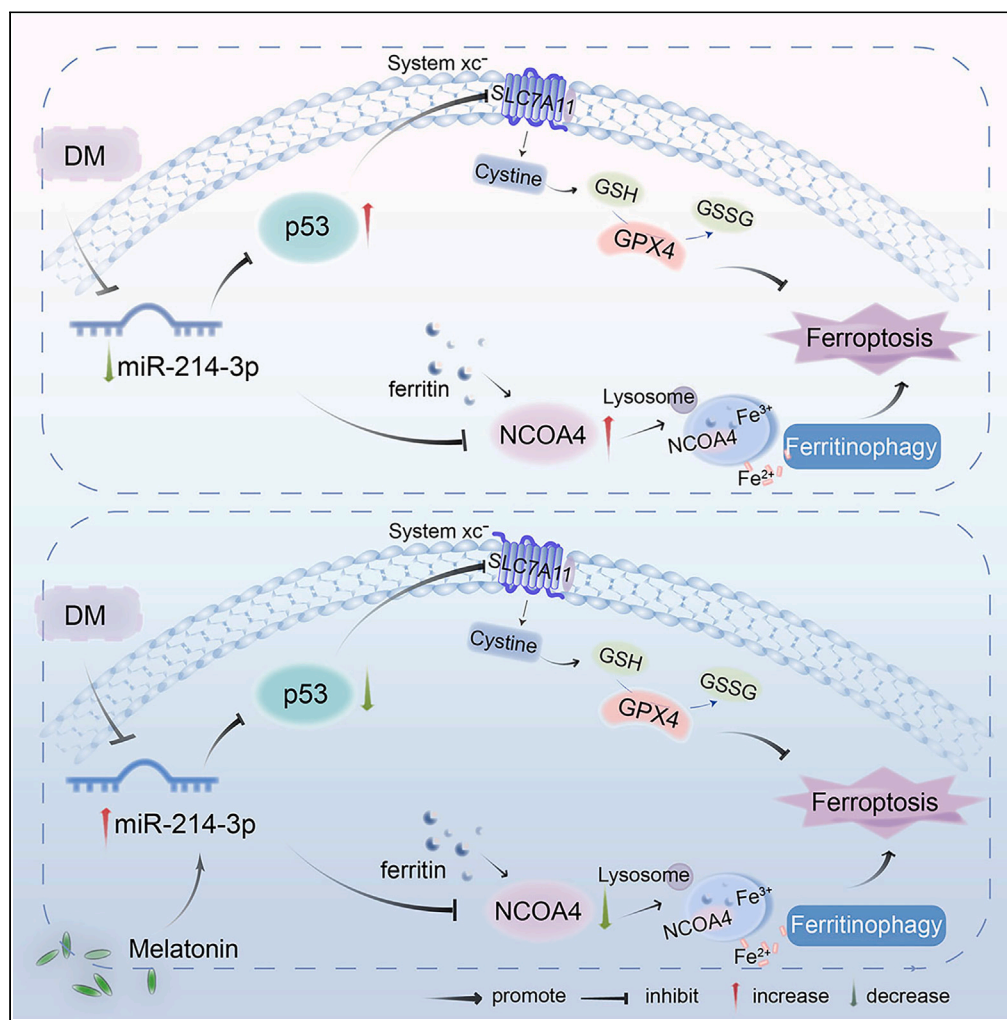


Article

A mechanism linking ferroptosis and ferritinophagy in melatonin-related improvement of diabetic brain injury



Jiaojiao Yu, Yu Zhang, Qin Zhu, ..., Han Meng, Jun Han, Hui Che

hanjun@wnmc.edu.cn (J.H.)
chehui1203@163.com (H.C.)

Highlights

Ferroptosis and ferritinophagy activation contributes to diabetic brain injury

MiR-214-3p is involved in p53-mediated ferroptosis

MiR-214-3p is a negative regulator of NCOA4-mediated ferritinophagy

Melatonin inhibits neuronal ferroptosis and ferritinophagy via miR-214-3p



Article

A mechanism linking ferroptosis and ferritinophagy in melatonin-related improvement of diabetic brain injury

Jiaojiao Yu,^{1,9} Yu Zhang,^{1,6,9} Qin Zhu,^{1,9} Zhengrui Ren,¹ Mengting Wang,¹ Sasa Kong,¹ Hongbo Lv,⁷ Tao Xu,¹ Zhaoyu Xie,¹ Han Meng,¹ Jun Han,^{2,3,4,5,*} and Hui Che^{1,3,8,10,*}

SUMMARY

Ferroptosis and ferritinophagy play critical roles in various disease contexts. Herein, we observed that ferroptosis and ferritinophagy were induced both in the brains of mice with diabetes mellitus (DM) and neuronal cells after high glucose (HG) treatment, as evidenced by decreases in GPX4, SLC7A11, and ferritin levels, but increases in NCOA4 levels. Interestingly, melatonin administration ameliorated neuronal damage by inhibiting ferroptosis and ferritinophagy both *in vivo* and *in vitro*. At the molecular level, we found that not only the ferroptosis inducer p53 but also the ferritinophagy mediator NCOA4 was the potential target of miR-214-3p, which was downregulated by DM status or HG insult, but was increased after melatonin treatment. However, the inhibitory effects of melatonin on ferroptosis and ferritinophagy were blocked by miR-214-3p downregulation. These findings suggest that melatonin is a potential drug for improving diabetic brain damage by inhibiting p53-mediated ferroptosis and NCOA4-mediated ferritinophagy through regulating miR-214-3p in neurons.

INTRODUCTION

Diabetes mellitus (DM) is a group of chronic metabolism disorders that is characterized by hyperglycemia. It was reported that 536 million people suffered from DM in 2021, and this number will increase to 783 million in 2045 worldwide.¹ DM contributes to numerous organ injuries.^{2–4} Previous studies have indicated that DM leads to multiple brain injuries, such as neurodegeneration, white matter damage, brain infarction, cognitive deficits, or dementia.^{5–7} Despite substantial advancements in the understanding of this pathophysiological process, no effective target-oriented drugs or therapeutic strategies are available for treating brain injury under DM conditions. Therefore, it is necessary to further explore the potential molecular mechanism involved and identify effective therapeutic drugs for improving brain injury induced by DM.

Previous studies have demonstrated that neuronal cell death is involved in DM-induced brain injury.^{8–10} Ferroptosis, a novel type of regulated cell death, is triggered by excessive iron accumulation and lipid peroxidation. In general, it can occur mainly via extrinsic or intrinsic pathways. The extrinsic pathway is driven by system x_c^- , which contributes to glutathione (GSH) synthesis. The intrinsic pathway is induced by the inhibition of antioxidant enzymes, such as glutathione peroxidase 4 (GPX4). Blocking solute carrier family 7 member 11 (SLC7A11), which is a critical subunit of system x_c^- , can result in GPX4 inactivation through GSH depletion, thereby triggering lipid peroxidation-mediated ferroptosis.^{11,12} Previous studies have reported that p53 is involved in triggering ferroptotic cell death by inhibiting SLC7A11.¹³ In addition to p53, ferritinophagy is also involved in promoting ferroptosis. Ferritinophagy, mediated by nuclear receptor co-activator 4 (NCOA4), contributes to the degradation of ferritin, thereby triggering the release of Fe^{2+} into cells and lipid peroxidation, ultimately promoting ferroptosis.¹⁴ Emerging evidence has revealed that ferroptosis and ferritinophagy participate in the pathological processes of various diseases, including diabetes and its complications.^{15–20} However, it is not yet clear whether ferroptosis and ferritinophagy are associated with brain injury under DM conditions and how ferroptosis and ferritinophagy are inhibited to protect against diabetic brain injury.

¹Department of Pharmacology, School of Pharmacy, Wannan Medical College, Wuhu, China

²Anhui College of Traditional Chinese Medicine, Wuhu, China

³Anhui Innovative Center for Drug Basic Research of Metabolic Diseases, Wannan Medical College, Wuhu, China

⁴Anhui Provincial Engineering Laboratory for Screening and Re-evaluation of Active Compounds of Herbal Medicines in Southern Anhui, Wannan Medical College, Wuhu, China

⁵Anhui Provincial Engineering Research Center for Polysaccharide Drugs, Wannan Medical College, Wuhu, China

⁶Department of Geriatrics, The Second Affiliated Hospital of Harbin Medical University, Harbin, China

⁷School of Anesthesia, Wannan Medical College, Wuhu, China

⁸Department of Endocrinology and Genetic Metabolism, The First Affiliated Hospital of Wannan Medical College (Yijishan Hospital of Wannan Medical College), Wuhu, China

⁹These authors contributed equally

¹⁰Lead contact

*Correspondence: hanjun@wnmc.edu.cn (J.H.), chehui1203@163.com (H.C.)

<https://doi.org/10.1016/j.isci.2024.109511>



Melatonin is a kind of hormone that is synthesized mainly by the pineal gland. Emerging evidence has indicated that melatonin has beneficial effects on treating brain injury induced by diverse pathological factors, such as traumatic brain injury, chronic cerebral hypoperfusion, subarachnoid hemorrhage, A β neurotoxicity, and aging.^{21–23} In addition, melatonin has been proven that is involved in the onset and progression of DM and diabetic complications. For example, melatonin is associated with improving DM-induced cardiac injury by regulating SIRT6.²⁴ Melatonin alleviates diabetic kidney injury through influencing the SIRT1/Nrf2/HO-1 axis.²⁵ As did other studies, our previous study showed that melatonin could alleviate DM-induced brain injury by inhibiting neuronal autophagy and pyroptosis.²⁶ However, to our knowledge, there have been no reports about the function of melatonin on ferroptosis and ferritinophagy during the pathogenesis of DM-induced brain injury.

In the present study, we found that melatonin protected against neuronal ferroptosis and ferritinophagy by regulating the miR-214-3p/p53 and miR-214-3p/NCOA4 axes, respectively, suggesting that the neuroprotective effect of melatonin on diabetic brain injury is, at least in part, dependent on inhibiting ferroptotic cell death.

RESULTS

Melatonin attenuates DM-induced ferroptosis

Emerging evidence has indicated that ferroptosis contributes to different types of brain damage. Our previous study showed that melatonin improved DM-induced brain injury by inhibiting neuronal death; therefore, we asked ourselves whether the neuroprotective effect of melatonin was associated with regulating neuronal ferroptosis in the brains of STZ-induced mice. As shown in Figures 1A–1D, melatonin administration obviously decreased the number of injured neurons in the DM group detected by Nissl and FJC staining assays. Moreover, the level of LDH was markedly increased in the brains of STZ-induced DM mice, but it was reversed by melatonin administration (Figure 1E). Furthermore, we observed changes in ferroptosis-related markers in the brains of mice with DM that were treated with or without melatonin. As shown in Figures 1F and 1G, an increase in MDA level accompanied with a decrease in GSH and SOD levels were observed in the brains of the DM group. Interestingly, these changes were reversed by melatonin treatment. Likewise, ferroptosis-related proteins, such as SLC7A11 and GPX4, were markedly reduced by DM. However, melatonin treatment significantly upregulated the abovementioned proteins (Figure 1H). Similar changes in GPX4 were further identified by immunohistochemistry assay (Figure 1I). These data suggest that melatonin partly rescues DM-induced brain injury by inhibiting neuronal ferroptosis.

Melatonin inhibits neuronal ferroptosis under HG conditions

Next, we further ascertained the role of melatonin in neuronal ferroptosis using an experimental cell model. Cell viability was decreased by high glucose (HG) insult, which was reversed by melatonin treatment (Figure 2A). Additionally, melatonin reversed the HG-induced increase in LDH level in neuronal cells (Figure 2B). The Calcein-AM/EthD-III assay indicated that melatonin inhibited the cell death induced by HG treatment (Figure 2C). Consistent with the *in vivo* results, HG treatment induced the levels of MDA but reduced the levels of GSH and SOD in neuronal cells. Importantly, these lipid-peroxidation-associated changes were reversed by melatonin treatment (Figures 2D–2F). Moreover, the transmission electron microscopy results showed that HG insult resulted in mitochondrial atrophy and mitochondrial ridge disappearance. These findings were reversed by melatonin treatment (Figure 2G). As illustrated in Figure 2H, the protein expressions of SLC7A11 and GPX4 were lower in HG-treated neurons than in control neurons, and these changes were abolished by melatonin treatment. Importantly, we found that melatonin-mediated ferroptosis inhibition was abolished by Erastin treatment, a ferroptosis inducer, but further increased by treatment with Ferrostatin-1, a ferroptosis inhibitor (Figures 2I and 2J). These results indicate that melatonin contributes to inhibiting ferroptosis in neuronal cells treated with HG.

The anti-ferroptotic effect of melatonin is associated with regulating miR-214-3p/p53 axis

Based on our foregoing findings both *in vivo* and *in vitro*, we next aimed to investigate how melatonin regulates neuronal ferroptosis and the potential molecular mechanism involved. Our previous report showed that melatonin inhibited neuronal autophagy and pyroptosis by regulating miR-214-3p expression under DM conditions. These findings prompted us to hypothesize whether miR-214-3p is associated with melatonin-mediated neuronal ferroptosis inhibition. Treatment with AMO-214-3p, a miR-214-3p inhibitor, reduced the level of miR-214-3p in HG-treated neuronal cells after melatonin treatment (Figure 3A). As shown in Figures 3B and 3C, Calcein-AM/EthD-III and CCK-8 assays revealed that miR-214-3p downregulation abolished the inhibitory effect of melatonin on cell death under HG conditions. In addition, miR-214-3p inhibition blunted the neuroprotective effect of melatonin on HG-treated neuronal cells (Figure 3D). Intriguingly, compared with melatonin treatment alone, downregulation of miR-214-3p had the opposite effect on the levels of SOD and GSH (Figures 3E and 3F). Moreover, an increase in SLC7A11 and GPX4 protein expressions was blocked by AMO-214-3p under HG conditions after melatonin treatment (Figure 3G). Similar results were obtained by immunofluorescence assay (Figures 3H and 3I). Intriguingly, we found that the expression of both SLC7A11 and GPX4 were downregulated by AMO-214-3p, whereas they were upregulated by miR-214-3p under normal conditions (Figures 4A and 4B). Similar observations were obtained from the immunofluorescence assay (Figures 4C and 4D).

Despite the previous data indicating that the melatonin-mediated inhibition of neuronal ferroptosis might be ascribed to the regulation of miR-214-3p expression, the direct downstream target of miR-214-3p is worth exploring. Earlier studies reported that p53 is not only involved in promoting ferroptosis through the suppression of SLC7A11 but also a potential downstream target of miR-214-3p.^{13,27} Thus, we hypothesized that the miR-214-3p-mediated regulation of neuronal ferroptosis might be associated with the modulation of p53 expression. As anticipated,

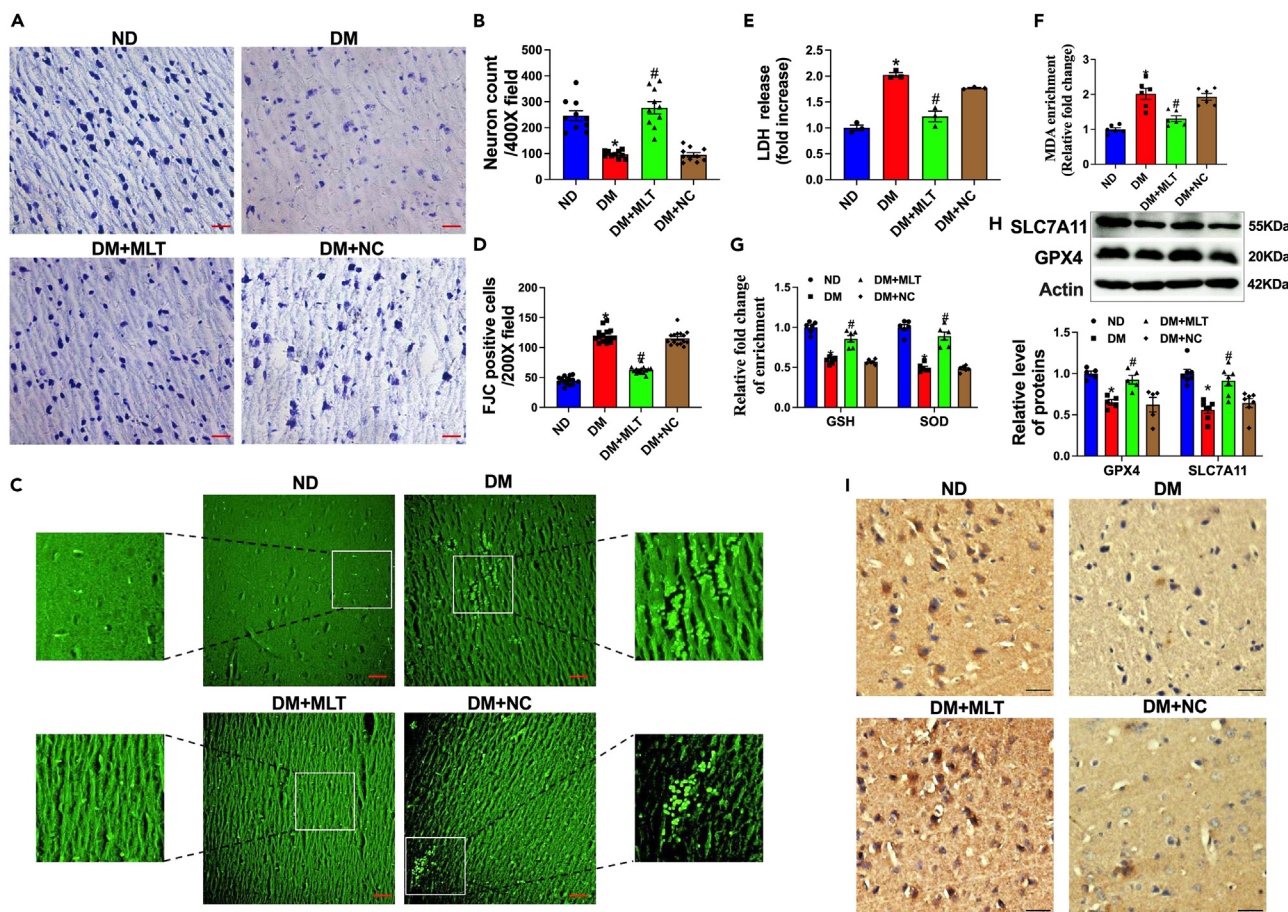


Figure 1. Melatonin attenuates DM-induced ferroptosis

(A and B) Nissl staining of DM-induced neuronal damage after melatonin administration. $n = 10$ randomly selected areas were calculated. Scale bar: $50 \mu\text{m}$.

(C and D) FJC staining showing melatonin decreased DM-induced damaged neurons. $n = 15$ randomly selected areas were calculated. Scale bar: $20 \mu\text{m}$.

(E) Melatonin reduced LDH release in STZ mice. $n = 3$ in each group.

(F and G) Detection of MDA, GSH, and SOD in different groups. $n = 6$ in each group.

(H) The levels of SLC7A11 and GPX4 were detected by western blotting. $n = 5-7$ in each group.

(I) IHC staining of GPX4. Scale bar: $50 \mu\text{m}$ * $p < 0.05$ vs. ND. # $p < 0.05$ vs. DM. Data are represented as mean \pm SEM. ND, nondiabetic; DM, diabetes mellitus; MLT, melatonin; NC, negative control.

we observed that the expression of p53 was reduced by miR-214-3p, whereas it was induced by AMO-214-3p (Figure 4E). A similar result was confirmed by an immunofluorescence assay (Figure 4F). As shown in Figures 5A–5C, the protein level of p53 was markedly increased in the brains of DM mice, which was significantly reduced by melatonin treatment. However, the mRNA level of p53 did not change in response to melatonin treatment. Importantly, we found that the melatonin-induced decrease in p53 was blocked by antagonomiR-214-3p transfection. The immunohistochemistry results were consistent (Figure 5D). As illustrated in Figure 5E, HG insult led to an increase in p53 protein expression. Similar to the results *in vivo*, melatonin treatment reduced the HG-induced increase in p53, and this effect was blocked by miR-214-3p inhibition (Figures 5F and 5G). These results at least in part indicate that miR-214-3p/p53 axis is associated with melatonin-inhibited neuronal ferroptosis.

Melatonin alleviates neuronal ferritinophagy both *in vivo* and *in vitro*

Accumulating evidence from our group and others has demonstrated that dysfunctional neuronal autophagy plays a vital role in improving DM-induced brain damage, and melatonin exerts anti-autophagy effects under different pathological conditions.²⁶ Ferritinophagy is a new form of autophagic-ferroptosis that is mediated by NCOA4 and contributes to promoting ferroptosis activation by degrading ferritin and inducing iron accumulation.¹⁴ These findings prompted us to hypothesize whether melatonin participates in modulating neuronal ferritinophagy. To test this hypothesis, we first detected changes in ferritinophagy-related proteins, including NCOA4 and ferritin. As illustrated in Figures 6A and 6B, the protein level of NCOA4 was markedly increased in the DM group, whereas the change in ferritin showed the opposite trend. Importantly, these changes were abolished after melatonin treatment. However, changes in NCOA4 protein expression in the brains

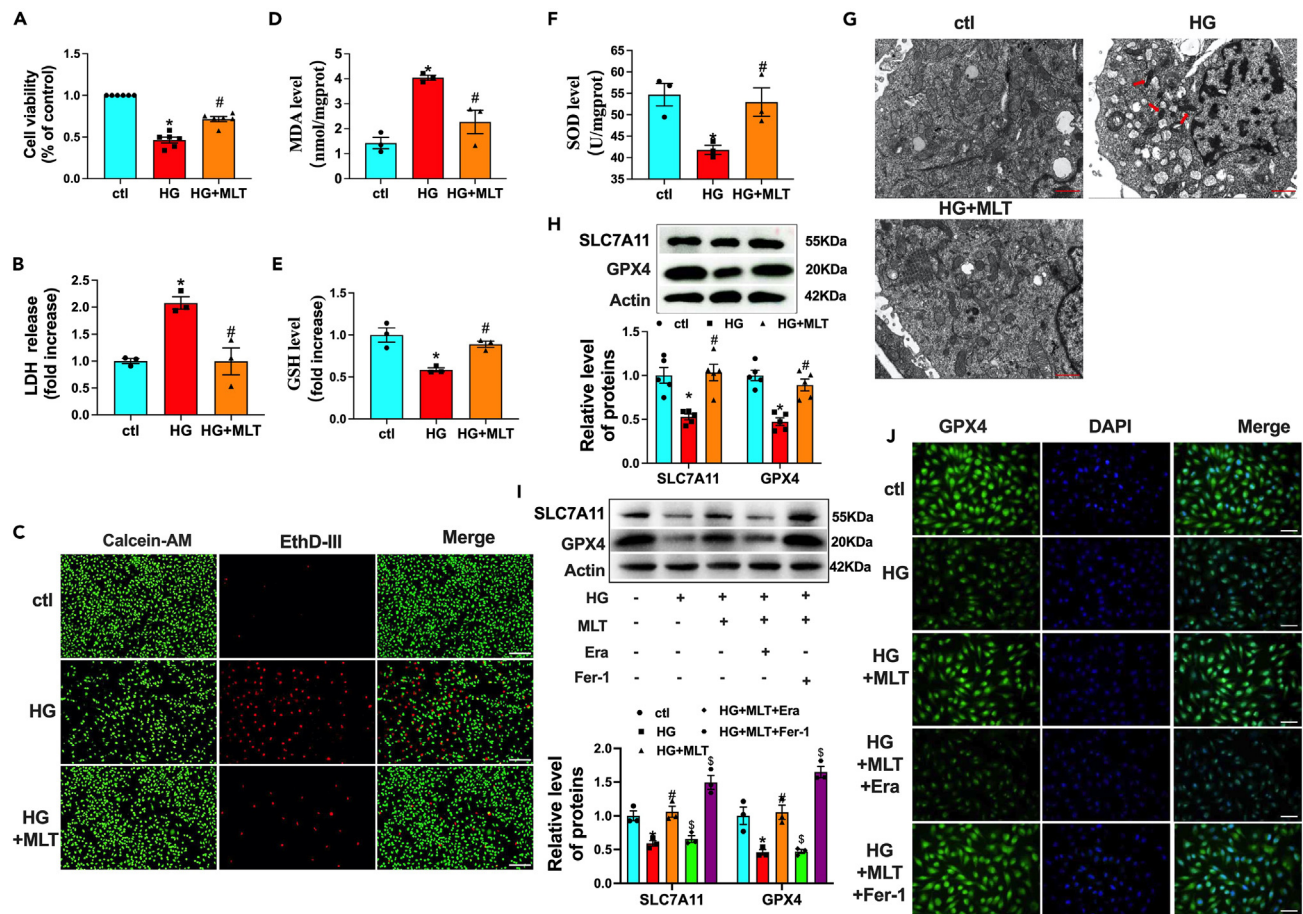


Figure 2. Melatonin inhibits neuronal ferroptosis under high-glucose conditions (A–C) Cell viability under different conditions was detected by CCK-8, LDH, and calcein-AM/EthD-III assays. n = 3–6 per group. Scale bar: 100 μ m. (D–F) The levels of MDA, GSH, and SOD were detected in SH-SY5Y cells. n = 3 per group. (G) The ultrastructural changes in SH-SY5Y cells were detected by TEM. Red arrowheads indicate mitochondrial atrophy and the disappearance of the mitochondrial ridge. Scale bar: 1 μ m. (H and I) Western blotting was used to detect the levels of SLC7A11 and GPX4 in SH-SY5Y cells. n = 3–5 per group. (J) The expression of GPX4 was detected by IF staining. Scale bar: 20 μ m. *p < 0.05 vs. ctl, #p < 0.05 vs. HG, §p < 0.05 vs. HG + MLT. Data are represented as mean \pm SEM. ctl, control; HG, high glucose; Era, Erastin; Fer-1, Ferrostatin-1.

were not due to an increase in NCOA4 mRNA in response to melatonin treatment (Figure 6C). The contents of Fe²⁺ and total iron were induced in the DM group. However, melatonin administration abolished these changes (Figure 6D). As illustrated in Figures 6E–6G, melatonin reversed the HG-induced upregulation of NCOA4 and downregulation of ferritin expression in neuronal cells similar with the *in vivo* data. Moreover, HG treatment induced higher contents of Fe²⁺ and total iron relative to those in control cells, and these changes were partly blunted after melatonin treatment (Figure 6H). Furthermore, the effect of melatonin on NCOA4 under HG conditions was abolished by rapamycin, an autophagy inducer (Figures 6I and 6J). These results suggest that melatonin is associated with the inhibition of neuronal ferritinophagy.

Melatonin exerts antiferritinophagy effects by regulating the miR-214-3p/NCOA4 axis

Our foregoing results suggested that melatonin inhibits ferroptosis by regulating miR-214-3p; however, whether miR-214-3p is involved in melatonin-mediated ferritinophagy inhibition is unclear. As shown in Figure 7A, *Ncoa4*, a critical ferritinophagy-related gene, may be a candidate site of miR-214-3p predicted by TargetScan database. The activity of luciferase vector, containing binding sites between miR-214-3p and *Ncoa4* 3'UTR, was inhibited by miR-214-3p mimics, but miR-214-3p had no effect once the binding sites were mutated. However, cotransfection of AMO-214-3p increased the luciferase activity. The level of endogenous miR-214-3p was changed after transfected by miR-214-3p mimics and AMO-214-3p (Figure 7B). As illustrated in Figures 7C and 7D, the protein expression of NCOA4 was significantly decreased by miR-214-3p overexpression. However, knockdown of miR-214-3p resulted in NCOA4 upregulation. A similar change in NCOA4 induced by miR-214-3p was further identified using immunofluorescence assays (Figures 7E and 7F).

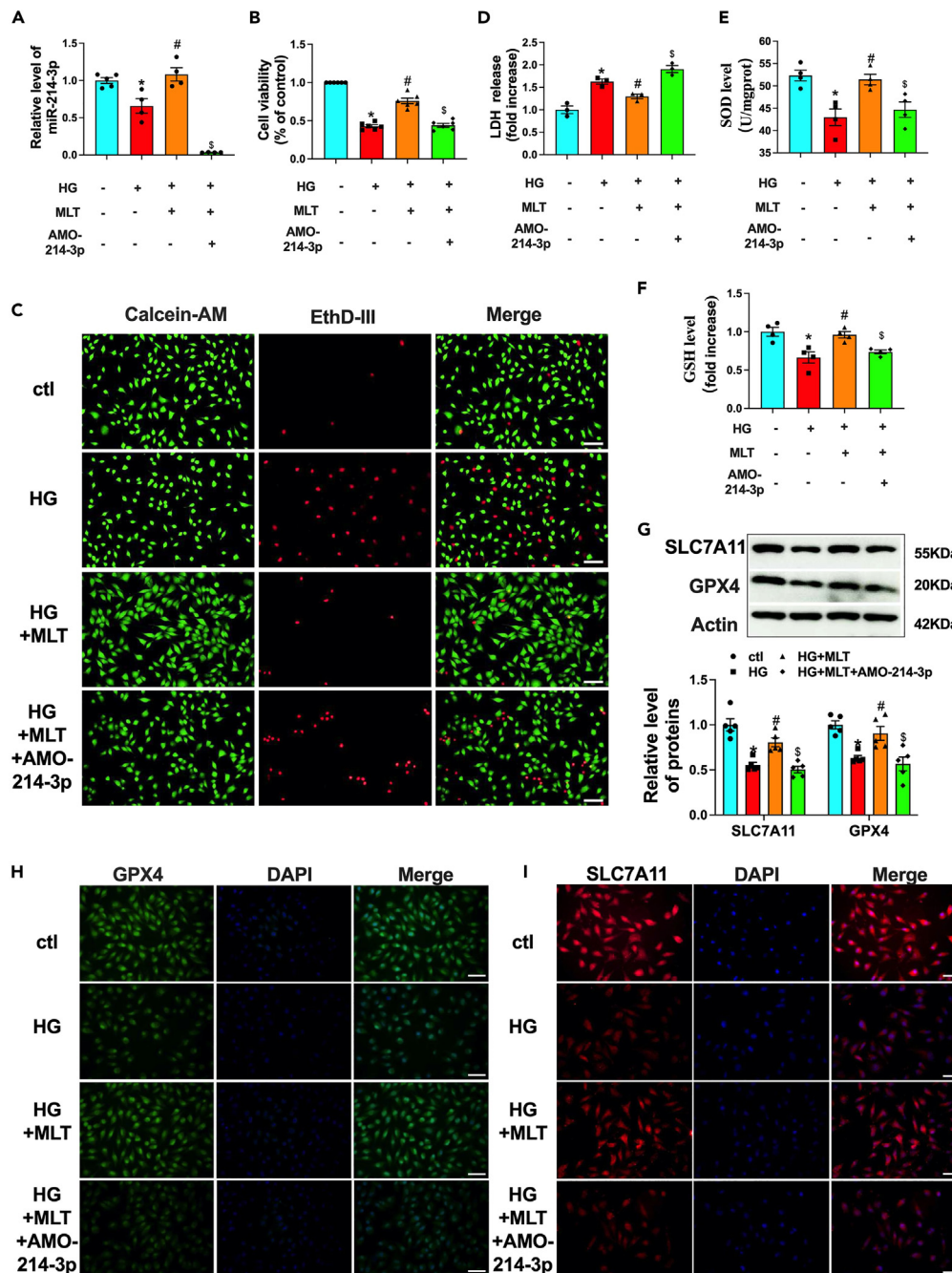


Figure 3. Effect of miR-214-3p on melatonin-related ferroptosis inhibition

(A) The change of miR-214-3p was detected by RT-qPCR assay. n = 4–5 in each group.

(B–D) CCK-8, calcein-AM/EthD-III, and LDH assays were used to detect cell viability. n = 3–6 in each group. Scale bar: 50 μ m.

(E and F) The change of SOD and GSH was detected. n = 4 in each group.

(G) Western blotting was used to detect the change of GPX4 and SLC7A11. n = 5 in each group.

(H and I) IF staining of GPX4 and SLC7A11 in SH-SY5Y cells. *p < 0.05 vs. ctl, #p < 0.05 vs. HG, §p < 0.05 vs. HG + MLT. Data are represented as mean \pm SEM. AMO-214-3p: miR-214-3p inhibitor.

Moreover, we also observed that miR-214-3p inhibition caused a significant increase in Fe²⁺ level. The melatonin-induced decreases in the levels of Fe²⁺ and total iron were abolished by miR-214-3p inhibition under HG conditions (Figures 8A and 8B). Importantly, we found that the effect of melatonin on NCOA4 after HG treatment was blocked by miR-214-3p downregulation (Figures 8C and 8D). Moreover, AMO-214-3p blunted the effect of melatonin on ferritin in the context of HG (Figures 8E and 8F). Previous studies have shown that ferritin can be degraded

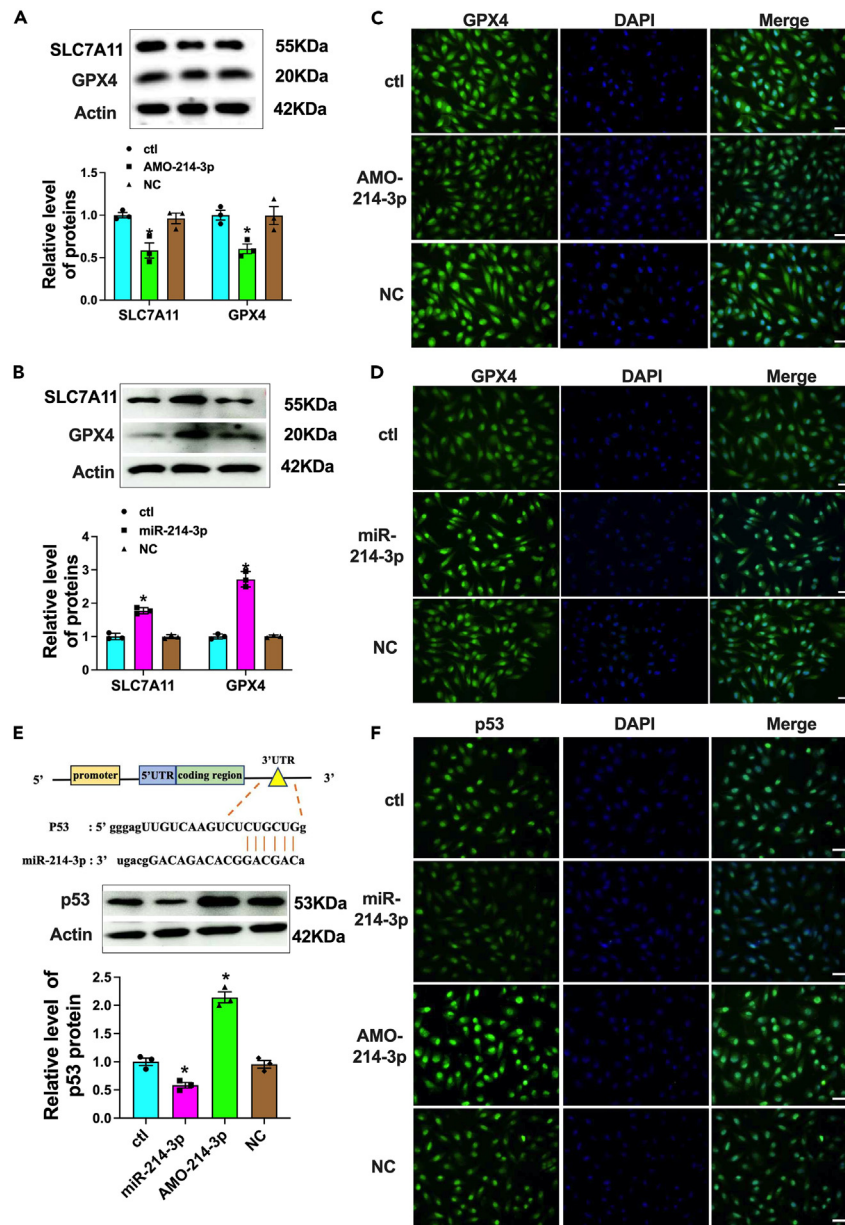


Figure 4. Effect of miR-214-3p on the expression of ferroptosis-associated proteins and its target of p53

(A) The change of SLC7A11 and GPX4 protein were detected by western blotting after AMO-214-3p transfection. n = 3 in each group.

(B) Western blotting was used to detect the expression of SLC7A11 and GPX4 after miR-214-3p transfection. n = 3 in each group.

(C and D) IF staining of GPX4 after transfecting with AMO-214-3p or miR-214-3p. (E) Top: complementarity of the binding sites between the miR-214-3p and p53 3'UTR. Bottom: western blotting of p53 protein after transfecting with AMO-214-3p or miR-214-3p. n = 3 in each group.

(F) IF staining for p53 in the different groups. Scale bar: 20 μ m *p < 0.05 vs. ctl. Data are represented as mean \pm SEM. NC: negative control.

in lysosomes through a process mediated by its interaction with NCOA4.²⁸ First, we confirmed that NCOA4 could interact with ferritin under HG conditions, which was blocked by melatonin treatment, but was reversed by downregulation of miR-214-3p (Figure 9A). To further determine the influence of miR-214-3p on NCOA4-mediated ferritinophagy in response to melatonin treatment, we costained ferritin and LAMP1, a marker of lysosomes, and found that the colocalization of endogenous ferritin and LAMP1 was decreased by melatonin treatment under HG conditions, whereas miR-214-3p inhibition induced an increase in the amount of ferritin bound to LAMP1 (Figure 9B). In addition, we detected the colocalization of ferritin with LC3, a marker of autophagy. Immunofluorescence analysis revealed that ferritin colocalized with LC3 under HG conditions, and this effect further increased by AMO-214-3p transfection (Figure 9C). Overall, these findings suggest that melatonin-related ferritinophagic inhibition is, at least in part, associated with regulating the miR-214-3p/NCOA4 axis.

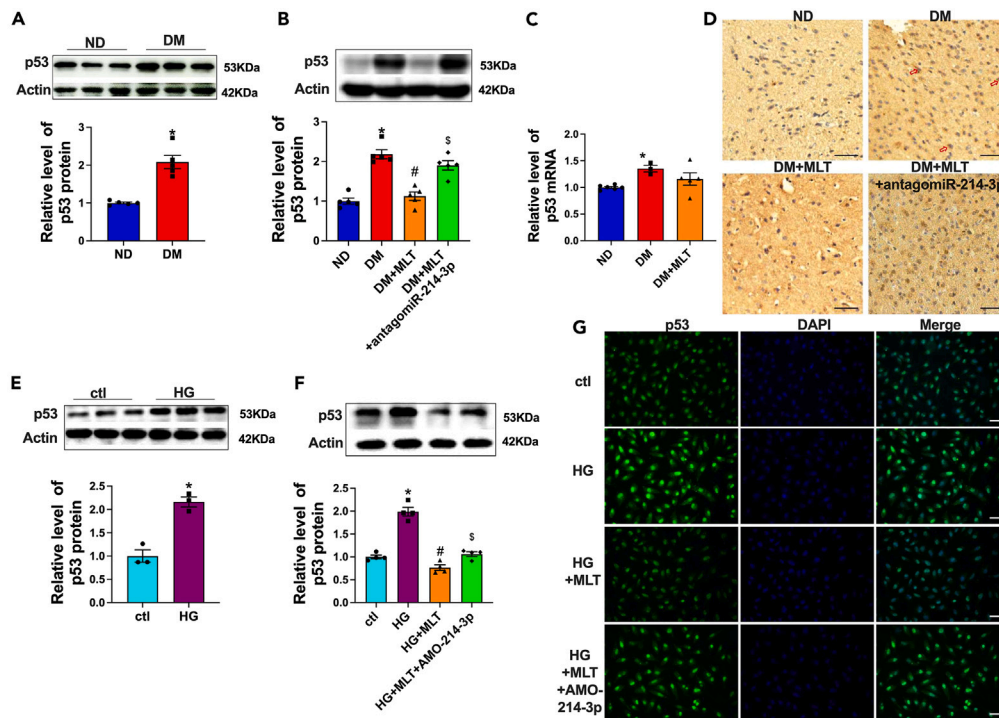


Figure 5. The antiferroptotic effect of melatonin is associated with modulation of the miR-214-3p/p53 axis

(A and B) The protein changes of p53 were analyzed by western blotting. n = 5 in each group.

(C) p53 mRNA level was detected by qPCR. n = 3–6 in each group.

(D) IHC staining was conducted to measure p53 expression. Scale bar: 50 μ m.

(E and F) Western blotting was used to detect p53 expression in SH-SY5Y cells. n = 3–4 in each group.

(G) IF staining for p53 in the SH-SY5Y cells. Scale bar: 20 μ m *p < 0.05 vs. ND or ctrl, #p < 0.05 vs. DM or HG, \$p < 0.05 vs. DM + MLT or HG + MLT. Data are represented as mean \pm SEM.

DISCUSSION

Ferroptosis, a novel identified form of cell death, plays a critical role in various pathological conditions, including diabetic brain injury. For example, Tang et al. reported that inhibiting neuronal ferroptosis could attenuate diabetic brain injury.²⁹ Hao et al. reported that Slc40a1-mediated ferroptosis was associated with the progression of cognitive dysfunction in type 1 diabetes patients.³⁰ Subsequently, Xie et al. reported that AMPK activation could improve cognitive function by inhibiting hippocampal ferroptosis in diabetic mice.³¹ However, whether the neuroprotective effect of melatonin on diabetic brain injury is associated with modulating neuronal ferroptosis has still not been determined. It is well known that blocking SLC7A11 can induce ferroptosis by triggering GSH inhibition and GPX4 inactivation. Therefore, it is necessary to assess whether ferroptosis occurs through lipid peroxidation. Herein, we found that DM resulted in neuronal ferroptosis, as demonstrated by decreases in the levels of GPX4, SLC7A11, and GSH in both diabetic mice induced by STZ injection and neuronal cells treated by HG. Moreover, we observed that the expression of other putative biomarkers of ferroptosis, such as MDA and SOD, significantly changed both *in vivo* and *in vitro*, and these changes were similar to those observed in previous studies.^{32–34} As expected, melatonin administration markedly reversed these ferroptosis-related changes and significantly attenuated neuronal damage *in vivo* and *in vitro*. Importantly, we observed that pretreatment with Erastin, an inducer of ferroptosis, abolished the function of melatonin on neuronal ferroptosis. Overall, melatonin-inhibited neuronal ferroptosis was further enhanced by Ferrostatin-1, an inhibitor of ferroptosis. These data suggested that melatonin partly contributed to the inhibition of neuronal ferroptosis.

Iron metabolism dysfunction participates in the occurrence and development of diabetes and its complications.^{35–38} Iron overload is another characteristic of ferroptosis in some specific contexts. Ferritinophagy is associated with promoting ferroptosis through the degradation of ferritin to release Fe²⁺, resulting in iron overload and lipid peroxidation. The inhibition of ferritinophagy contributes to ameliorating ferroptosis in various diseases.^{39–41} Increasing evidence has shown that ferritinophagy is mediated by NCOA4. However, there have been no reports about the relationship between NCOA4-mediated ferritinophagy and diabetic brain injury. Intriguingly, in our present study, we innovatively showed that DM resulted in NCOA4-mediated ferritinophagy activation, as demonstrated by increases in NCOA4, Fe²⁺, and total iron levels, along with the decrease in ferritin levels in both diabetic mice and neuronal cells after HG insult. Ferritinophagy is a special type of autophagy that is responsible for promoting ferroptosis by inducing lysosomal dysfunction.⁴² Our previous study has reported that the inhibitory effect of melatonin on autophagy could protect against brain injury induced by DM.²⁶ Therefore, we also determined whether the

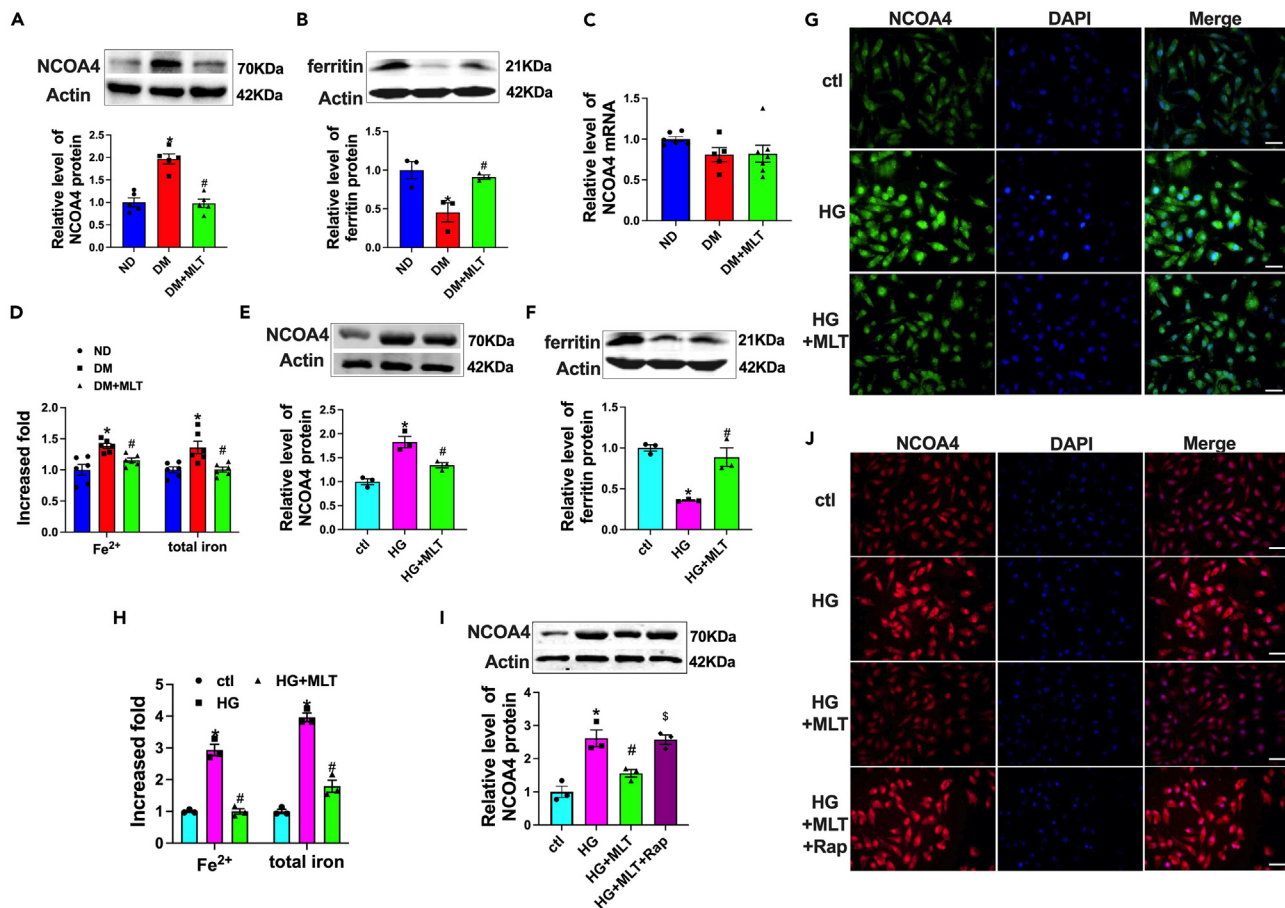


Figure 6. Effect of melatonin on neuronal ferritinophagy both *in vivo* and *in vitro*

(A and B) The changes of NCOA4 and ferritin were detected by western blotting in STZ mice brains with or without melatonin treatment. n = 3–5 in each group.

(C) RT-qPCR was used to detect the mRNA of NCOA4. n = 5–7 per group.

(D) The total iron and Fe²⁺ levels were examined in STZ mice brains with or without melatonin treatment. n = 6 in each group.

(E and F) Western blotting was used to measure the levels of NCOA4 and ferritin. n = 3 in each group.

(G) IF staining of NCOA4. Scale bar: 20 μ m.

(H) The total iron and Fe²⁺ levels were examined in SH-SY5Y cells after HG treatment. n = 3 in each group.

(I and J) Western blotting and IF staining were used to measure NCOA4 expression. n = 3 in each group. Scale bar: 20 μ m *p < 0.05 vs. ND or ctrl, #p < 0.05 vs. DM or HG, \$p < 0.05 vs. DM + MLT or HG + MLT; data are represented as mean \pm SEM. Rap, rapamycin.

neuroprotective effect of melatonin on diabetic brain injury was associated with modulating NCOA4-dependent ferritinophagy. As expected, we found that these changes, increase in NCOA4, Fe²⁺, and total iron levels and decrease in ferritin levels, were reversed by melatonin administration both *in vivo* and *in vitro*. It has been reported that the interaction of NCOA4 with ferritin is essential for ferritinophagy to promote ferroptosis.²⁸ Knockdown of NCOA4 inhibits ferroptosis by reducing ferritin degradation.⁴³ Consistent with these early studies, our results revealed that melatonin treatment blocks the increase in the colocalization of endogenous ferritin and NCOA4 under HG conditions. Two markers of autophagy, LAMP1 for lysosomes and LC3 for autophagosomes, were used to further demonstrate the effect of melatonin on ferritinophagy. Moreover, melatonin treatment decreased the colocalization of endogenous ferritin and LAMP1 after HG insult. Moreover, the interaction between ferritin and LC3 was blocked by melatonin treatment. These results indicated that melatonin also partly contributed to the inhibition of NCOA4-mediated ferritinophagy in the brain in the context of DM.

Our foregoing data further provide the biological evidence for the potential ability of melatonin to ameliorate diabetic brain injury associated not only with neuronal ferroptosis but also with ferritinophagy. Previous studies have reported that melatonin regulates ferroptosis by regulating protein-coding genes. However, whether noncoding RNAs are associated with melatonin-inhibited neuronal ferroptosis under DM conditions has not been determined. Our findings herein showed that the protein level of NCOA4 was decreased by melatonin, but melatonin had no such effect on NCOA4 mRNA. Even though DM could increase the protein and mRNA levels of p53, melatonin treatment decreased only the p53 protein level without affecting the p53 mRNA level, suggesting that the mechanism of posttranscriptional regulation might be involved in the process of melatonin-inhibited ferritinophagy and ferroptosis. MicroRNA-214-3p (miR-214-3p) is a class of noncoding RNA that

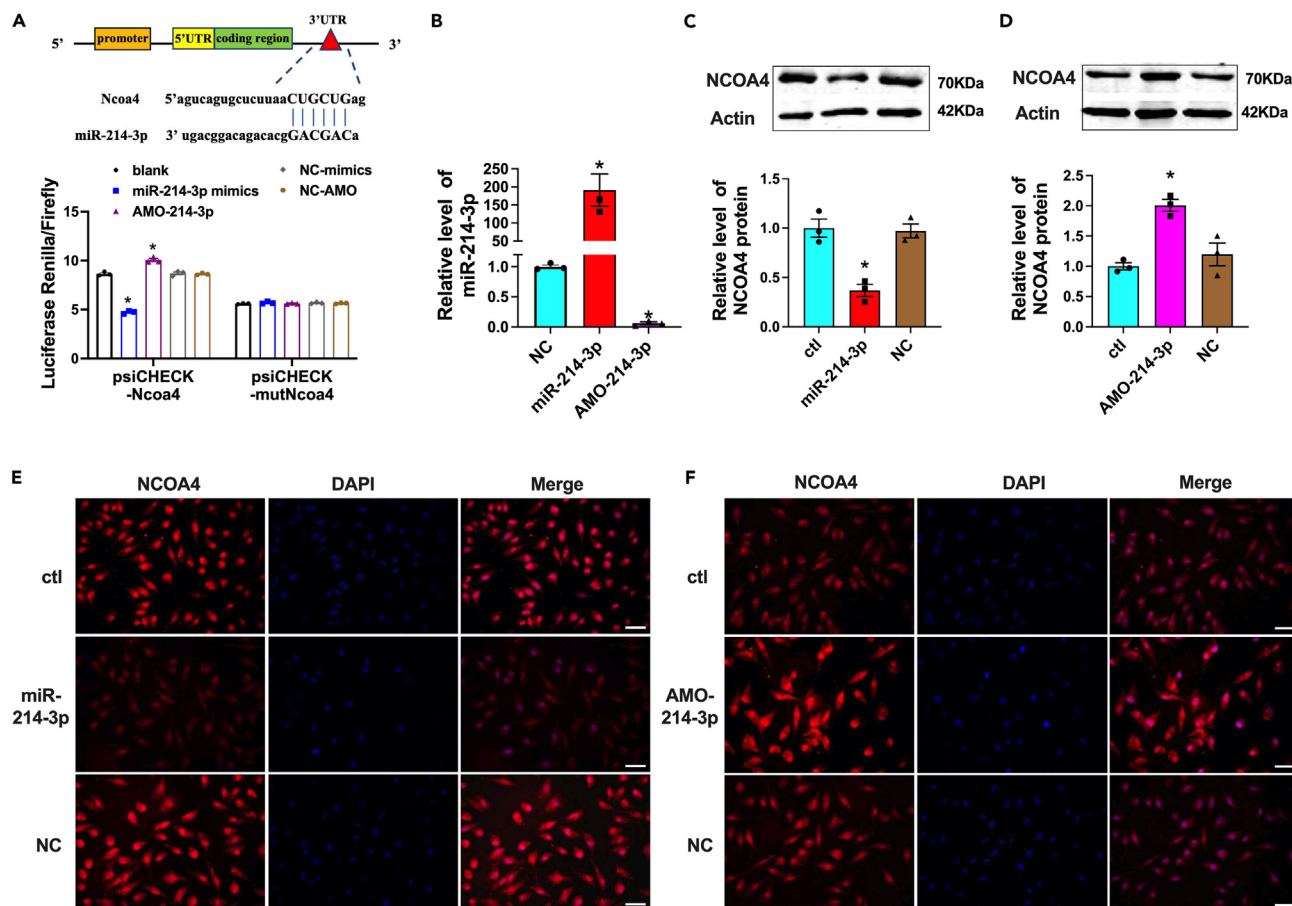


Figure 7. MiR-214-3p regulates NCOA4 expression in neuronal cells

(A) Top: bioinformatics plot showing that there are complementary binding sites between the miR-214-3p and Ncoa4 3'UTR according to the TargetScan algorithm. Bottom: effects of miR-214-3p on luciferase activity in cells containing wild-type binding sites (left panel) or mutant binding sites (right panel). n = 3 in each group.

(B) RT-qPCR assay was used to detect miR-214-3p level. n = 3 in each group.

(C and D) The change of NCOA4 was measured by western blotting after transfecting miR-214-3p or AMO-214-3p. n = 3 in each group.

(E and F) IF staining of NCOA4 in cells. Scale bar: 20 μ m *p < 0.05 vs. ctl. Data are represented as mean \pm SEM.

contributes to various pathophysiological processes of diseases by regulating target gene expression at the posttranscriptional level.^{44,45} Previously published data from other groups and our group have demonstrated that miR-214-3p is associated with the progression of diabetic complications, including diabetic brain injury.^{26,46–48} Therefore, in the present study, we selected miR-214-3p as a potential noncoding RNA to investigate the underlying molecular mechanism of melatonin in neuronal ferritinophagy and ferroptosis. As expected, we proposed the finding that NCOA4 is a candidate target of miR-214-3p and found that overexpression of miR-214-3p reduced NCOA4 levels and downstream Fe²⁺ and total iron levels, as well as induced ferritin levels. However, miR-214-3p knockdown induced the reverse changes. Importantly, we observed that the beneficial effect of melatonin on neuronal NCOA4-mediated ferritinophagy was abolished by miR-214-3p inhibition, as evidenced by the reversal of the interaction of ferritin with NCOA4, the induction of colocalization of endogenous ferritin and LAMP1, and the increase in the amount of ferritin bound to LC3, suggesting that melatonin protects against diabetic brain injury through regulating NCOA4-mediated ferritinophagy by regulating miR-214-3p.

According to various molecular mechanisms, p53 is considered to promote ferroptosis by limiting cysteine uptake through the negative regulation of SLC7A11 transcription.¹³ Earlier studies reported that the expression of p53 in the brain was greater in patients suffering from DM than in nondiabetic patients.⁴⁹ Importantly, miR-214-3p could regulate the expression of p53 in cancer cells.²⁷ Based on these data and the findings of other studies, we propose the hypothesis that miR-214-3p mediates neuronal ferroptosis through regulating p53 expression during the progression of brain injury induced by DM. As expected, we found that miR-214-3p could negatively regulate the expression of p53 in neuronal cells. Importantly, we found that the inhibitory effect of melatonin on neuronal ferroptosis was abolished by the downregulation of miR-214-3p. These data suggest that melatonin reduces neuronal p53-mediated ferroptosis at least in part by regulating miR-214-3p.

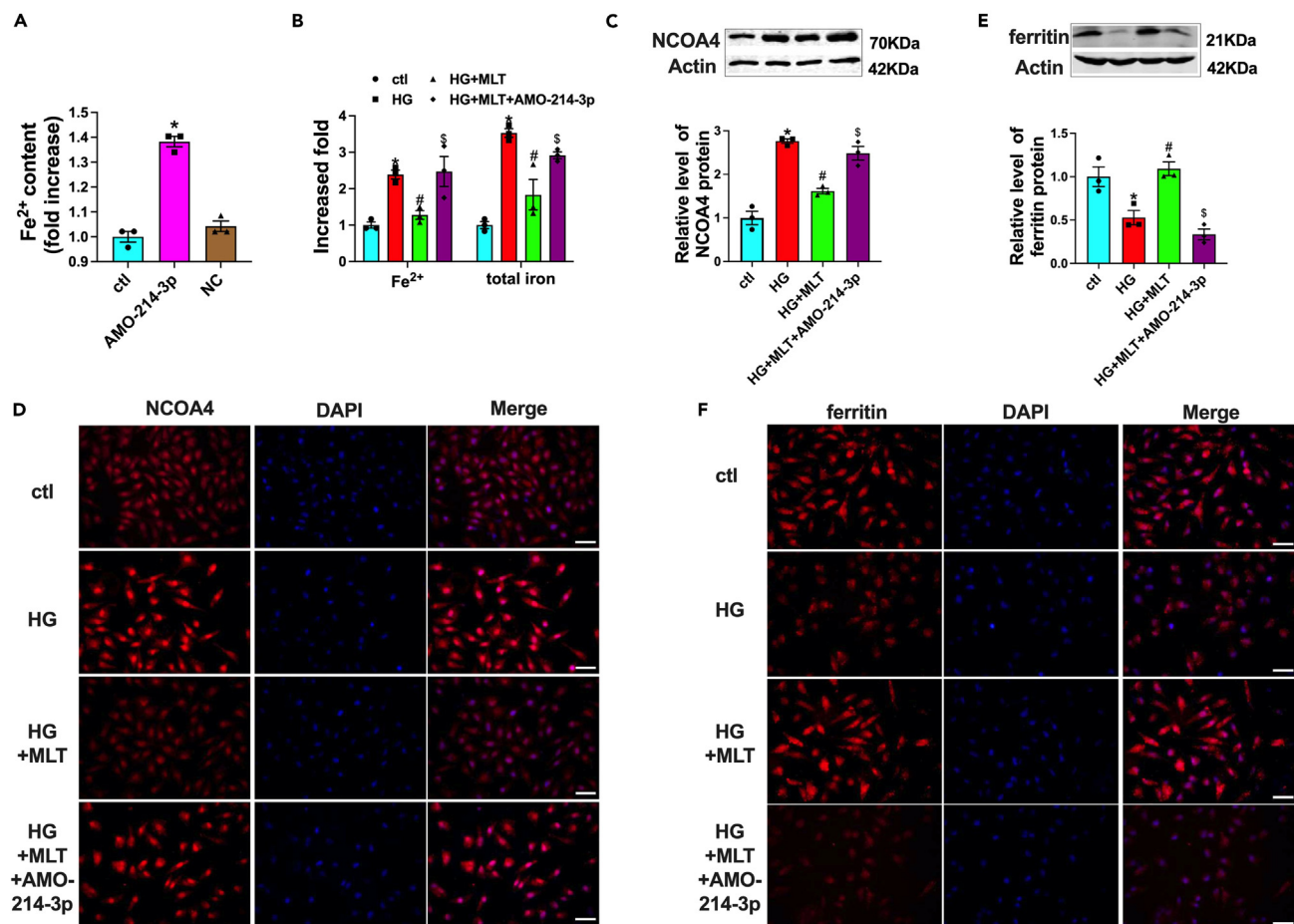


Figure 8. Melatonin exerts antiferritinophagy effects through targeting the miR-214-3p/NCOA4 axis

(A) Fe²⁺ levels were increased in SH-SY5Y neuronal cells after AMO-214-3p transfection. n = 3 in each group.

(B) The Fe²⁺ and total iron were measured by iron kits. n = 3 in each group.

(C and D) The changes of NCOA4 were detected by western blotting and IF staining assays. n = 3 in each group. Scale bar: 20 μ m.

(E and F) The level of ferritin were analyzed by western blotting and IF staining assays. n = 3 in each group. Scale bar: 20 μ m. *p < 0.05 vs. ctrl, #p < 0.05 vs. HG, ^sp < 0.05 vs. HG + MLT. Data are represented as mean \pm SEM.

In summary, we identified a new molecular mechanism for the neuroprotective effect role of melatonin in the context of diabetic brain injury: melatonin protects against brain injury by suppressing neuronal ferroptosis and ferritinophagy. At the molecular level, evidence suggests that miR-214-3p is a common regulator of ferroptosis and ferritinophagy. Specifically, melatonin exerts its antiferroptotic and antiferritinophagy effects by regulating the miR-214-3p/p53 axis and the miR-214-3p/NCOA4 pathway, respectively.

Limitations of the study

In this study, although we have demonstrated that melatonin could inhibit neuronal ferroptosis and ferritinophagy via regulating miR-214-3p, there are some limitations. One is that we could not exclude whether other miRNAs were involved in melatonin-related improvement of diabetic brain injury. In addition, we only used the pharmacological induced animal model of diabetes in this study; it should pay attention when the results from this study were translated to human condition. Moreover, only 8-week time point was selected; it would be interesting to identify the effect of melatonin on diabetic brain injury at different timepoints. Additionally, there is no separate group in which melatonin was intraperitoneally administered to the healthy mice. Although previous studies have demonstrated that melatonin did not exert antioxidant effect under control status, it is more rigorous to set up the group of melatonin alone as a control.

STAR METHODS

Detailed methods are provided in the online version of this paper and include the following:

- KEY RESOURCES TABLE
- RESOURCE AVAILABILITY

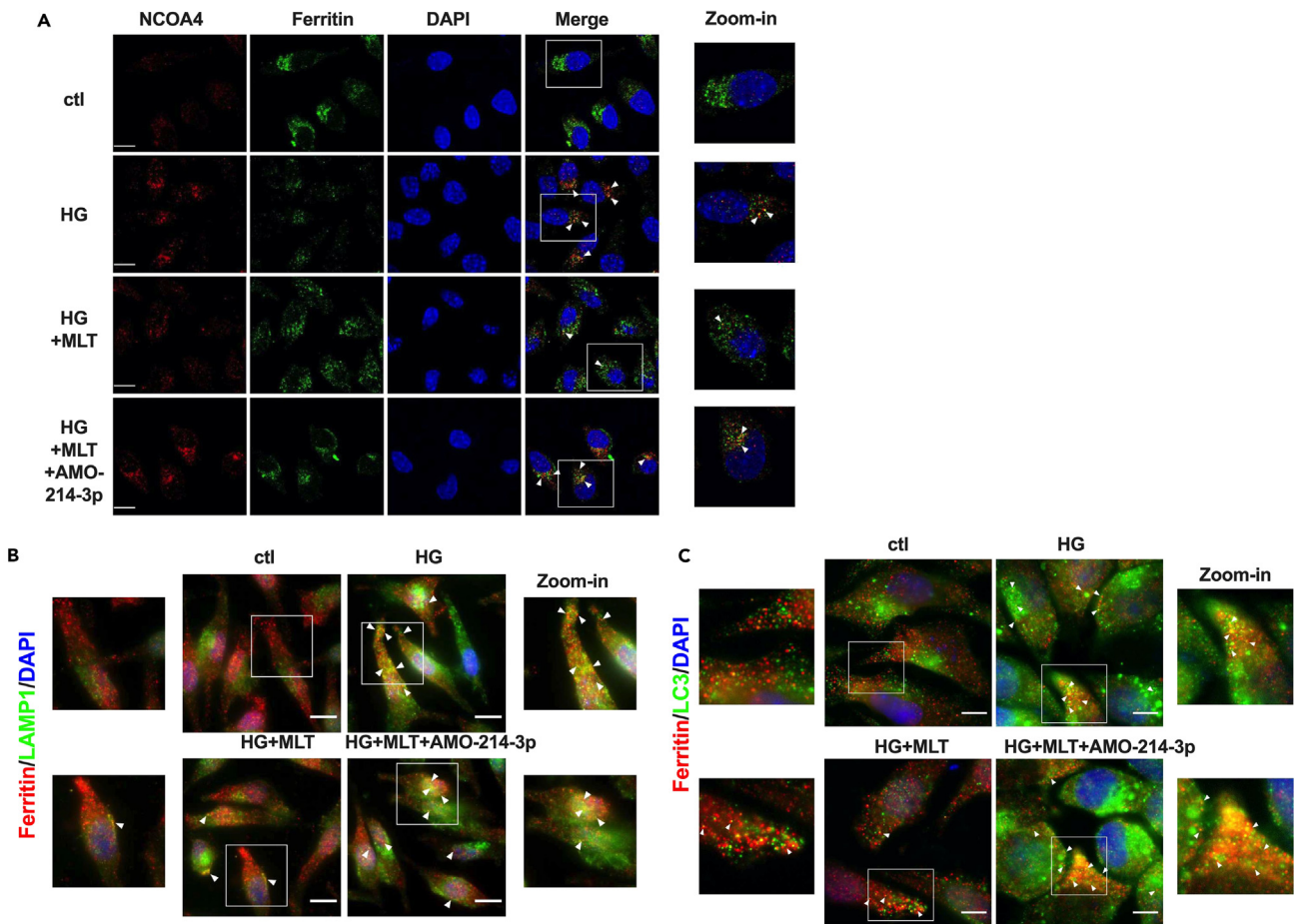


Figure 9. Effect of melatonin on colocalization of ferritinophagy-related proteins

(A) IF staining of ferritin (green) and NCOA4 (red) in SH-SY-5Y cells. Scale bar:10 μ m.

(B) The colocalization of ferritin (red) and LAMP1 (green) was detected by IF staining. Scale bar:10 μ m.

(C) IF staining of ferritin (red) and LC3 (green) in SH-SY-5Y cells. The white arrows indicate the possible colocalization. Scale bar: 5 μ m.

- Lead contact
- Materials availability
- Data and code availability
- **EXPERIMENTAL MODEL AND STUDY PARTICIPANT DETAILS**
 - Animal models establishment
 - Neuronal cell culture
- **METHOD DETAILS**
 - Drug treatment
 - Neuronal cell transfection and treatment
 - Nissl staining and Fluoro-Jade C (FJC) staining
 - Immunohistochemistry staining
 - Immunofluorescence staining
 - Cellular viability measurements
 - LDH assay
 - MDA, SOD and GSH measurements
 - Iron content determination
 - Western blotting analysis
 - qRT-PCR
 - Luciferase reporter assay
 - Transmission electron microscopy
- **QUANTIFICATION AND STATISTICAL ANALYSIS**

ACKNOWLEDGMENTS

This work was supported by the National Natural Science Foundation of China (grant number 82270879, Hui Che), Foundation of Excellent Youth Scholars of Education Committee of Anhui province of China (grant number 2022AH030124, Hui Che), and College Student Innovation and Entrepreneurship Training Program Project (grant number S202310368032, Hongbo Lv).

AUTHOR CONTRIBUTIONS

H.C. and J.H. contributed to design of the experiment and draft the manuscript; H.C., J.Y., and Y.Z. were involved in analysis of data. J.Y., Y.Z., Z.R., M.W., S.K., and T.X. performed the *in vivo* experiment. J.Y., Y.Z., Q.Z., H.L., H.M., and Z.X. contributed to the *in vitro* experiment. All authors have revised the draft critically.

DECLARATION OF INTERESTS

The authors declare no competing interests.

Received: September 12, 2023

Revised: January 1, 2024

Accepted: March 13, 2024

Published: March 15, 2024

REFERENCES

- Sun, H., Saeedi, P., Karuranga, S., Pinkepank, M., Ogurtsova, K., Duncan, B.B., Stein, C., Basit, A., Chan, J.C.N., Mbanya, J.C., et al. (2022). IDF Diabetes Atlas: Global, regional and country-level diabetes prevalence estimates for 2021 and projections for 2045. *Diabetes Res. Clin. Pract.* **183**, 109119.
- Schiborn, C., and Schulze, M.B. (2022). Precision prognostics for the development of complications in diabetes. *Diabetologia* **65**, 1867–1882.
- Ritchie, R.H., and Abel, E.D. (2020). Basic Mechanisms of Diabetic Heart Disease. *Circ. Res.* **126**, 1501–1525.
- Tan, T.E., and Wong, T.Y. (2022). Diabetic retinopathy: Looking forward to 2030. *Front. Endocrinol.* **13**, 1077669.
- Hamed, S.A. (2017). Brain injury with diabetes mellitus: evidence, mechanisms and treatment implications. *Expet Rev. Clin. Pharmacol.* **10**, 409–428.
- Zhang, Y., Zhang, X., Zhang, J., Liu, C., Yuan, Q., Yin, X., Wei, L., Cui, J., Tao, R., Wei, P., and Wang, J. (2014). Gray matter volume abnormalities in type 2 diabetes mellitus with and without mild cognitive impairment. *Neurosci. Lett.* **562**, 1–6.
- Kodl, C.T., Franc, D.T., Rao, J.P., Anderson, F.S., Thomas, W., Mueller, B.A., Lim, K.O., and Seagquist, E.R. (2008). Diffusion tensor imaging identifies deficits in white matter microstructure in subjects with type 1 diabetes that correlate with reduced neurocognitive function. *Diabetes* **57**, 3083–3089.
- Kong, F.J., Ma, L.L., Guo, J.J., Xu, L.H., Li, Y., and Qu, S. (2018). Endoplasmic reticulum stress/autophagy pathway is involved in diabetes-induced neuronal apoptosis and cognitive decline in mice. *Clin. Sci.* **132**, 111–125.
- Muriach, M., Flores-Bellver, M., Romero, F.J., and Barcia, J.M. (2014). Diabetes and the brain: oxidative stress, inflammation, and autophagy. *Oxid. Med. Cell. Longev.* **2014**, 102158.
- Liu, L., Wang, N., Kalionis, B., Xia, S., and He, Q. (2022). HMGB1 plays an important role in pyroptosis induced blood brain barrier breakdown in diabetes-associated cognitive decline. *J. Neuroimmunol.* **362**, 577763.
- Chen, X., Kang, R., Kroemer, G., and Tang, D. (2021). Broadening horizons: the role of ferroptosis in cancer. *Nat. Rev. Clin. Oncol.* **18**, 280–296.
- Tang, D., Chen, X., Kang, R., and Kroemer, G. (2021). Ferroptosis: molecular mechanisms and health implications. *Cell Res.* **31**, 107–125.
- Liu, D.S., Duong, C.P., Haupt, S., Montgomery, K.G., House, C.M., Azar, W.J., Pearson, H.B., Fisher, O.M., Read, M., Guerra, G.R., et al. (2017). Inhibiting the system Xc⁻/glutathione axis selectively targets cancers with mutant-p53 accumulation. *Nat. Commun.* **8**, 14844.
- Santana-Codina, N., Gikandi, A., and Mancias, J.D. (2021). The Role of NCOA4-Mediated Ferritinophagy in Ferroptosis. *Adv. Exp. Med. Biol.* **1301**, 41–57.
- Jiang, X., Stockwell, B.R., and Conrad, M. (2021). Ferroptosis: mechanisms, biology and role in disease. *Nat. Rev. Mol. Cell Biol.* **22**, 266–282.
- Sun, Y., Guo, L.Q., Wang, D.G., Xing, Y.J., Bai, Y.P., Zhang, T., Wang, W., Zhou, S.M., Yao, X.M., Cheng, J.H., et al. (2023). Metformin alleviates glucolipotoxicity-induced pancreatic β cell ferroptosis through regulation of the GPX4/ACSL4 axis. *Eur. J. Pharmacol.* **956**, 175967.
- Miao, R., Fang, X., Zhang, Y., Wei, J., Zhang, Y., and Tian, J. (2023). Iron metabolism and ferroptosis in type 2 diabetes mellitus and complications: mechanisms and therapeutic opportunities. *Cell Death Dis.* **14**, 186.
- Wang, X., Chen, X., Zhou, W., Men, H., Bao, T., Sun, Y., Wang, Q., Tan, Y., Keller, B.B., Tong, Q., et al. (2022). Ferroptosis is essential for diabetic cardiomyopathy and is prevented by sulforaphane via AMPK/NRF2 pathways. *Acta Pharm. Sin. B* **12**, 708–722.
- Sun, Y., Bai, Y.P., Wang, D.G., Xing, Y.J., Zhang, T., Wang, W., Zhou, S.M., Cheng, J.H., Chang, W.W., Kong, X., et al. (2023). Protective effects of metformin on pancreatic beta-cell ferroptosis in type 2 diabetes *in vivo*. *Biomed. Pharmacother.* **168**, 115835.
- Qu, X.F., Liang, T.Y., Wu, D.G., Lai, N.S., Deng, R.M., Ma, C., Li, X., Li, H.Y., Liu, Y.Z., Shen, H.T., and Chen, G. (2021). Acyl-CoA synthetase long chain family member 4 plays detrimental role in early brain injury after subarachnoid hemorrhage in rats by inducing ferroptosis. *CNS Neurosci. Ther.* **27**, 449–463.
- Wang, Z., Zhou, F., Dou, Y., Tian, X., Liu, C., Li, H., Shen, H., and Chen, G. (2018). Melatonin Alleviates Intracerebral Hemorrhage-Induced Secondary Brain Injury in Rats via Suppressing Apoptosis, Inflammation, Oxidative Stress, DNA Damage, and Mitochondria Injury. *Transl. Stroke Res.* **9**, 74–91.
- Chen, C., Yang, C., Wang, J., Huang, X., Yu, H., Li, S., Li, S., Zhang, Z., Liu, J., Yang, X., and Liu, G.P. (2021). Melatonin ameliorates cognitive deficits through improving mitophagy in a mouse model of Alzheimer's disease. *J. Pineal Res.* **71**, e12774.
- Shen, S., Liao, Q., Wong, Y.K., Chen, X., Yang, C., Xu, C., Sun, J., and Wang, J. (2022). The role of melatonin in the treatment of type 2 diabetes mellitus and Alzheimer's disease. *Int. J. Biol. Sci.* **18**, 983–994.
- Yu, L.M., Dong, X., Xue, X.D., Xu, S., Zhang, X., Xu, Y.L., Wang, Z.S., Wang, Y., Gao, H., Liang, Y.X., et al. (2021). Melatonin attenuates diabetic cardiomyopathy and reduces myocardial vulnerability to ischemia-reperfusion injury by improving mitochondrial quality control: Role of SIRT6. *J. Pineal Res.* **70**, e12698.
- Shi, S., Lei, S., Tang, C., Wang, K., and Xia, Z. (2019). Melatonin attenuates acute kidney ischemia/reperfusion injury in diabetic rats by activation of the SIRT1/Nrf2/HO-1 signaling pathway. *Biosci. Rep.* **39**, BSR20181614.
- Che, H., Li, H., Li, Y., Wang, Y.Q., Yang, Z.Y., Wang, R.L., and Wang, L.H. (2020). Melatonin exerts neuroprotective effects by inhibiting neuronal pyroptosis and autophagy in STZ-induced diabetic mice. *Faseb. J.* **34**, 14042–14054.
- Chandrasekaran, K.S., Sathyanarayanan, A., and Karunakaran, D. (2017). miR-214 activates TP53 but suppresses the expression of RELA, CTNBN1, and STAT3 in human cervical and

- colorectal cancer cells. *Cell Biochem. Funct.* 35, 464–471.
28. Liu, J., Kuang, F., Kroemer, G., Klionsky, D.J., Kang, R., and Tang, D. (2020). Autophagy-Dependent Ferroptosis: Machinery and Regulation. *Cell Chem. Biol.* 27, 420–435.
 29. Tang, W., Li, Y., He, S., Jiang, T., Wang, N., Du, M., Cheng, B., Gao, W., Li, Y., and Wang, Q. (2022). Caveolin-1 Alleviates Diabetes-Associated Cognitive Dysfunction Through Modulating Neuronal Ferroptosis-Mediated Mitochondrial Homeostasis. *Antioxidants Redox Signal.* 37, 867–886.
 30. Hao, L., Mi, J., Song, L., Guo, Y., Li, Y., Yin, Y., and Zhang, C. (2021). SLC40A1 Mediates Ferroptosis and Cognitive Dysfunction in Type 1 Diabetes. *Neuroscience* 463, 216–226.
 31. Xie, Z., Wang, X., Luo, X., Yan, J., Zhang, J., Sun, R., Luo, A., and Li, S. (2023). Activated AMPK mitigates diabetes-related cognitive dysfunction by inhibiting hippocampal ferroptosis. *Biochem. Pharmacol.* 207, 115374.
 32. Liang, D., Minikes, A.M., and Jiang, X. (2022). Ferroptosis at the intersection of lipid metabolism and cellular signaling. *Mol. Cell* 82, 2215–2227.
 33. Chen, J., Guo, P., Han, M., Chen, K., Qin, J., and Yang, F. (2023). Cognitive protection of sinomenine in type 2 diabetes mellitus through regulating the EGF/Nrf2/HO-1 signaling, the microbiota-gut-brain axis, and hippocampal neuron ferroptosis. *Phytother Res.* 37, 3323–3341.
 34. Guo, T., Yu, Y., Yan, W., Zhang, M., Yi, X., Liu, N., Cui, X., Wei, X., Sun, Y., Wang, Z., et al. (2023). Erythropoietin ameliorates cognitive dysfunction in mice with type 2 diabetes mellitus via inhibiting iron overload and ferroptosis. *Exp. Neurol.* 365, 114414.
 35. Deng, H., Wei, J., Min, K., Yang, H., Wang, S., Xiao, Z., Liu, M., Zheng, L., Zhou, H., Chen, Y., et al. (2023). Research trends in ferroptosis since the origin of the concept: A bibliometric analysis. *Clin. Exp. Pharmacol. Physiol.* 50, 149–157.
 36. Zhang, T., Wang, M.Y., Wang, G.D., Lv, Q.Y., Huang, Y.Q., Zhang, P., Wang, W., Zhang, Y., Bai, Y.P., and Guo, L.Q. (2024). Metformin improves nonalcoholic fatty liver disease in db/db mice by inhibiting ferroptosis. *Eur. J. Pharmacol.* 966, 176341.
 37. Chen, Y., Li, S., Yin, M., Li, Y., Chen, C., Zhang, J., Sun, K., Kong, X., Chen, Z., and Qian, J. (2023). Isorhapontigenin Attenuates Cardiac Microvascular Injury in Diabetes via the Inhibition of Mitochondria-Associated Ferroptosis Through PRDX2-MFN2-ACSL4 Pathways. *Diabetes* 72, 389–404.
 38. Wang, H., Liu, D., Zheng, B., Yang, Y., Qiao, Y., Li, S., Pan, S., Liu, Y., Feng, Q., and Liu, Z. (2023). Emerging Role of Ferroptosis in Diabetic Kidney Disease: Molecular Mechanisms and Therapeutic Opportunities. *Int. J. Biol. Sci.* 19, 2678–2694.
 39. Santana-Codina, N., and Mancias, J.D. (2018). The Role of NCOA4-Mediated Ferritinophagy in Health and Disease. *Pharmaceuticals* 11, 114.
 40. Quiles Del Rey, M., Mancias, J.D., and Mancias, J.D. (2019). NCOA4-Mediated Ferritinophagy: A Potential Link to Neurodegeneration. *Front. Neurosci.* 13, 238.
 41. Li, W., Li, W., Wang, Y., Leng, Y., and Xia, Z. (2021). Inhibition of DNMT-1 alleviates ferroptosis through NCOA4 mediated ferritinophagy during diabetes myocardial ischemia/reperfusion injury. *Cell Death Dis.* 7, 267.
 42. Dowdle, W.E., Nyfeler, B., Nagel, J., Elling, R.A., Liu, S., Triantafellow, E., Menon, S., Wang, Z., Honda, A., Pardee, G., et al. (2014). Selective VPS34 inhibitor blocks autophagy and uncovers a role for NCOA4 in ferritin degradation and iron homeostasis in vivo. *Nat. Cell Biol.* 16, 1069–1079.
 43. Yu, F., Zhang, Q., Liu, H., Liu, J., Yang, S., Luo, X., Liu, W., Zheng, H., Liu, Q., Cui, Y., et al. (2022). Dynamic O-GlcNAcylation coordinates ferritinophagy and mitophagy to activate Ferroptosis. *Cell Discov.* 8, 40.
 44. Li, D., Liu, J., Guo, B., Liang, C., Dang, L., Lu, C., He, X., Cheung, H.Y.S., Xu, L., Lu, C., et al. (2016). Osteoclast-derived exosomal miR-214-3p inhibits osteoblastic bone formation. *Nat. Commun.* 7, 10872.
 45. Wang, X., Guo, B., Li, Q., Peng, J., Yang, Z., Wang, A., Li, D., Hou, Z., Lv, K., Kan, G., et al. (2013). miR-214 targets ATF4 to inhibit bone formation. *Nat. Med.* 19, 93–100.
 46. Pang, B., Qiao, L., Wang, S., Guo, X., Xie, Y., and Han, L. (2021). MiR-214-3p plays a protective role in diabetic neuropathic rats by regulating Nav1.3 and TLR4. *Cell Biol. Int.* 45, 2294–2303.
 47. Ma, Z., Li, L., Livingston, M.J., Zhang, D., Mi, Q., Zhang, M., Ding, H.F., Huo, Y., Mei, C., and Dong, Z. (2020). p53/microRNA-214/ULK1 axis impairs renal tubular autophagy in diabetic kidney disease. *J. Clin. Invest.* 130, 5011–5026.
 48. Wang, R., Zhang, Y., Jin, F., Li, G., Sun, Y., and Wang, X. (2019). High-glucose-induced miR-214-3p inhibits BMSCs osteogenic differentiation in type 1 diabetes mellitus. *Cell Death Dis.* 5, 143.
 49. Kung, C.P., and Murphy, M.E. (2016). The role of the p53 tumor suppressor in metabolism and diabetes. *J. Endocrinol.* 231, R61–R75.

STAR★METHODS

KEY RESOURCES TABLE

REAGENT or RESOURCE	SOURCE	IDENTIFIER
Antibodies		
Mouse monoclonal anti-p53	Proteintech	Cat# 60283-2-Ig; RRID: AB_2881401
Rabbit monoclonal anti-GPX4	Abcam	Cat# ab125066; RRID:AB_10973901
Rabbit monoclonal anti-xct	Abcam	Cat# AB307601; RRID: AB_3094570
Rabbit monoclonal anti-Ferritin	Abcam	Cat# AB75973; RRID:AB_1310222
Rabbit polyclonal anti-NCOA4	Abcam	Cat# AB222071; RRID: AB_3094571
Mouse monoclonal anti-LC3	MBL	Cat# M152-3; RRID:AB_1279144
Mouse monoclonal anti-LAMP1	cell signaling	Cat# 15665; RRID:AB_2798750
beta Actin Antibody	Affinity	Cat# AF7018; RRID:AB_2839420
Chemicals, peptides, and recombinant proteins		
Streptozotocin	Sigma-Aldrich	Cat# S0130
Melatonin	Sigma-Aldrich	Cat# M5250
Erastin	MedChemExpress	Cat# HY-15763
Ferrostatin-1	MedChemExpress	Cat# HY-100579
Rapamycin	MedChemExpress	Cat# AY-22989
Critical commercial assays		
FJC detection kit	Solarbio	Cat# G3262
CCK-8 kit	Biosharp	Cat# BS350B
Calcein-AM/EthD-III staining kit	BestBio	Cat# BB-41275
Lactate dehydrogenase(LDH) assay kit	njjcbio	Cat# A020-2-2
Reduced glutathione (GSH) assay kit	njjcbio	Cat# A006-2-1
Superoxide Dismutase (SOD) assay kit	njjcbio	Cat# A001-3-2
Cell Malondialdehyde (MDA) assay kit	njjcbio	Cat# A003-4-1
Iron Detection Kit	Jianglaibio	Cat# JL-T1116
Ferrous content detection kit	Jianglaibio	Cat# JL-T1255
ReverTra Ace qPCR RT Kit	Toyobo	Cat# FSQ-101
SYBR Green real-time PCR Master Mix Kit	Toyobo	Cat# QPK-201
Experimental models: Cell lines		
Human:SH-SY5Y cell line	ATCC	CRL-2266
Experimental models: Organisms/strains		
Mice:C57BL/6	Henan Sikebas Biotechnology Co., Ltd.	N/A
Oligonucleotides		
Mmu-U6-F ctcgcttcgagcagcacatatact	RiboBio	N/A
Mmu-U6-R acgcttcacgaattgctgtc	RiboBio	N/A
Mmu-miR-214-3p-F tatacatcaaacagcaggcaca	RiboBio	N/A
Mmu-miR-214-3p-R cattcgatctctccacagtctc	RiboBio	N/A
Software and algorithms		
Prism	Graph Pad	http://www.graphpad.com
ImageJ	NIH	https://imagej.nih.gov/ij/index.html

RESOURCE AVAILABILITY

Lead contact

Further information and requests for resources and reagents should be directed to and will be fulfilled by the lead contact, Hui Che (chehui1203@163.com).

Materials availability

This study did not generate new unique reagents.

Data and code availability

- All data reported in this paper will be shared by the [lead contact](#) upon request.
- This paper does not report original code.
- Any additional information required to reanalyze the data reported in this paper is available from the [lead contact](#) upon request.

EXPERIMENTAL MODEL AND STUDY PARTICIPANT DETAILS

Animal models establishment

C57BL/6 adult male mice (8 weeks old; weighing 20–22 g) were allowed *ad libitum* to obtain food and water, and housed at the temperature of $22 \pm 2^\circ\text{C}$ and $55 \pm 5\%$ relative humidity with a 12-h alternating dark/light cycle. To establish the model of DM, streptozotocin (60 mg/kg) was dissolved in 0.1 mol/L citrate buffer, and then intraperitoneally injected to the experimental mice for 3 consecutive days with food deprivation for 6–8 h each day. The mice were defined as DM when its fasting blood glucose level exceeded 16.7 mmol/L. The animal handling and experimental procedures were approved by the Laboratory Animals Ethical Committee of Wannan Medical College (approval no.LLSC-2022-166).

Neuronal cell culture

Neuronal cell lines SH-SY5Y were cultured in DMEM supplemented with 10% FBS and 1% antibiotics (penicillin and streptomycin) at 37°C in an incubator with 5% CO_2 .

METHOD DETAILS

Drug treatment

All experimental mice were randomly divided into non-diabetic (ND) group, diabetes mellitus (DM) group, and other groups as described in the [result](#) section ($n = 12$ per group). The 10 mg/kg of melatonin was orally administered to the DM mice once daily. After 8 weeks, the brain tissues from different groups were collected for the subsequent experiments.

Neuronal cell transfection and treatment

The glucose (33 mmol/L) was added into cells and maintained for 48 h to generate the DM model *in vitro*. For drug treatment, the cells received melatonin (10 μM), Erastin (1 μM), Ferrostatin-1 (1 μM) or Rapamycin (0.5 μM) at the same time as HG stimulation. For transfection, miR-214-3p mimics, AMO-214-3p or NC (RiboBio Co., Ltd., Guangzhou, China) were transfected into SH-SY5Y cells. The cells in the HG+melatonin+AMO-214-3p group were transfected with AMO-214-3p together with melatonin (10 μM) and subjected to HG treatment. After 48 h treatment, the cells were collected for subsequent experiments. All experiments were performed at least in triplicate.

Nissl staining and Fluoro-Jade C (FJC) staining

Mice were anesthetized by isoflurane (0.41 mL/min at 4L/min fresh gas flow), and then were transcardially perfused with 4% paraformaldehyde solution. The mice brains were isolated and embedded in paraffin. For Nissl staining, after deparaffinization and rehydration, the slices were incubated with cresyl violet, differentiated in Nissl differentiation solution, dehydrated with anhydrous ethanol, cleared with xylene, and then sealed with neutral gum. For FJC staining, the slices were immersed in different dilutions from the FJC detection kit. A total of 10–15 slices in each group were captured and the number of neurons in each slice were counted by using ImageJ software.

Immunohistochemistry staining

The mice brain from different group were cut into slices. After blocked with 10% normal goat serum, the primary antibodies of p53 (1:100) and GPX4 (1:500) were incubated overnight at 4°C . After incubated with the biotinylated secondary antibody, the slices were counterstained with haematoxylin, dehydrated under a range of alcohols, incubated with xylene, finally mounted with coverslips. All experiments were performed in triplicate.

Immunofluorescence staining

SH-SY5Y cells in different groups were fixed with 4% paraformaldehyde solution for 30 min. For penetrating and blocking, the cells were incubated with a special solution containing 10% goat serum and 0.3% Triton X-100. After that, the following primary antibodies were used: p53

(1:100), GPX4 (1:500), SLC7A11 (1:500), ferritin (1:500), NCOA4 (1:500), LC3 (1:500), and LAMP1 (1:100). After incubated with appropriate secondary antibodies, the cells were stained with DAPI for 15 min. All stained samples were imaged by using a fluorescence microscope. All experiments were performed in triplicate.

Cellular viability measurements

Cell viability was determined by CCK-8 kit and Calcein-AM/EthD-III staining kit. For CCK-8 assay, the absorbance at 450 nm was measured under a microplate reader. For Calcein-AM/EthD-III staining, the cells were seeded in 24-well plates. After corresponding treatment, 1 μ L/mL Calcein-AM was added at 37°C for 30 min. After that, 0.5 μ L/mL EthD-III was added for 3 min in the dark. The images were captured using a fluorescence microscope. All experiments were performed at least in triplicate.

LDH assay

The brain tissue was homogenized in physiological saline solution, and then the supernatants were obtained after centrifugation. The supernatants of SH-SY5Y cells were collected after melatonin or AMO-214-3p transfection with or without HG treatment. The level of LDH was measured following the corresponding manufacturing instructions. The absorbance was measured at 450 nm. All experiments were performed in triplicate.

MDA, SOD and GSH measurements

The brain tissue was homogenized in physiological saline solution, and then the supernatants were obtained after centrifugation. SH-SY5Y cells were digested by pancreatic enzymes after different treatments. After centrifugation, the precipitates were dissolved in PBS by ultrasonication. Afterward, GSH, SOD or MDA detection kits from njcbio were used following the corresponding manufacturing instructions. The absorbance was measured at 405 nm, 450 nm, or 532 nm. All experiments were performed at least in triplicate.

Iron content determination

The supernatants from tissue homogenates or cell samples were prepared following the corresponding manufacturing instructions. The levels of total iron and Fe²⁺ in the different groups were determined according to the instructions. The absorbance was detected at 562 nm. All experiments were performed at least in triplicate.

Western blotting analysis

Mice brain tissues or neuronal SH-SY5Y cells in the different treatment groups were lysed with RIPA buffer (Beyotime, Shanghai, China). The proteins were separated by SDS-PAGE, and transferred to NC membranes and blocked with 5% skim milk. The membranes were subsequently incubated with the following primary antibodies: p53 (1:2000), SLC7A11 (1:2000), GPX4 (1:1000), ferritin (1:1000), NCOA4 (1:1000) and β -actin (1:2000). The membranes were incubated with the corresponding secondary antibodies for 1 h. All protein bands were examined under a GelDoc XR System (Bio-Rad, USA) and analyzed with ImageJ software. All experiments were performed at least in triplicate.

qRT-PCR

Mouse brain tissues or neuronal SH-SY5Y cells from the different treatment groups were homogenized with TRIzol reagent to obtain total RNA. After that, cDNA were synthesized from 500 ng of RNA using a reverse transcription kit following the manufacturer's instructions. qPCR of the target genes was performed using SYBR Green reagent (Toyobo, Japan). The final data were calculated using the 2^{- $\Delta\Delta$ Ct} method after normalization against U6, which was chosen as the internal control. All experiments were performed at least in triplicate.

Luciferase reporter assay

The luciferase reporter plasmids were synthesized by using psi-CHECK2 vectors, containing wild-type or mutated binding sites between miR-214-3p and Ncoa4 3'UTR, after which the sequence of the plasmids was verified. HEK-293T cells were cultured at a density of approximately 40%–60% in DMEM. After that, different oligonucleotides (miR-214-3p, AMO-214-3p, or NC) were transfected with plasmids into cells. 48 h transfection later, the activity of luciferase reporter was examined according to the instructions (Promega). All experiments were performed at least in triplicate.

Transmission electron microscopy

The SH-SY5Y cells from different groups were isolated with 2.5% Trypsin-EDTA and centrifuged at 1000 rpm for 10 min. After that, cells were fixed with glutaraldehyde (2.5%) and osmium tetroxide (1%) at 4°C overnight. After dehydration, entrapment and double staining, the samples were observed under a transmission electron microscope (H-7650, Japan).

QUANTIFICATION AND STATISTICAL ANALYSIS

All the results are shown as the mean \pm SEM. Among multiple groups, statistical analysis was performed using ANOVA followed by Tukey's test. Student's t tests were used to analyze differences between two groups. $p < 0.05$ was considered to indicate statistical significance.